

# Lawrence Berkeley National Laboratory

## LBL Publications

### Title

Comparison of horace and photos Algorithms for Multiphoton Emission in the Context of W Boson Mass Measurement

### Permalink

<https://escholarship.org/uc/item/1sr4p2g2>

### Authors

Kotwal, Ashutosh V  
Jayatilaka, Bodhitha

### Publication Date

2016

### DOI

10.1155/2016/1615081

Peer reviewed

## Research Article

# Comparison of HORACE and PHOTOS Algorithms for Multiphoton Emission in the Context of $W$ Boson Mass Measurement

Ashutosh V. Kotwal<sup>1</sup> and Bodhitha Jayatilaka<sup>2</sup>

<sup>1</sup>Physics Department, Duke University, Durham, NC 27708, USA

<sup>2</sup>Scientific Computing Division, Fermi National Accelerator Laboratory, Batavia, IL 60510, USA

Correspondence should be addressed to Ashutosh V. Kotwal; ashutosh.kotwal@duke.edu

Received 21 October 2015; Accepted 24 December 2015

Academic Editor: Smarajit Triambak

Copyright © 2016 A. V. Kotwal and B. Jayatilaka. This is an open access article distributed under the Creative Commons Attribution License, which permits unrestricted use, distribution, and reproduction in any medium, provided the original work is properly cited. The publication of this article was funded by SCOAP<sup>3</sup>.

$W$  boson mass measurement is sensitive to QED radiative corrections due to virtual photon loops and real photon emission. The largest shift in the measured mass, which depends on the transverse momentum spectrum of the charged lepton from the boson decay, is caused by the emission of real photons from the final-state lepton. There are a number of calculations and codes available to model the final-state photon emission. We perform a detailed study, comparing the results from HORACE and PHOTOS implementations of the final-state multiphoton emission in the context of a direct measurement of  $W$  boson mass at Tevatron. Mass fits are performed using a simulation of the CDF II detector.

## 1. Introduction

The measurement of  $W$  boson mass ( $m_W$ ) is one of the most interesting precision electroweak observables. In the standard model (SM), the mass of  $W$  boson can be calculated with higher precision [1] than the existing measurement uncertainty [2–6], thus providing motivation for improving the statistical and systematic uncertainties on the measurement. The comparison between the theoretical prediction and the measurement provides a stringent test of the SM and constrains beyond-standard model (BSM) theories.

At hadron colliders, the mass of  $W$  boson is extracted from inclusively produced  $W$  bosons decaying to electrons or muons and the associated neutrinos. At the Tevatron, almost pure samples of such candidate events have been identified with backgrounds typically smaller than 1%. The momenta of the decay electrons and muons have been measured with a precision of  $\sim 0.01\%$ , allowing a  $W$  boson mass measurement with precision of 0.02% [6].

The calibration of the electron and muon momenta is the single most important aspect of the  $m_W$  measurement. In the approximation that  $W$  boson undergoes a two-body decay,

the distribution of the transverse momentum ( $p_T$ , defined as the component of the momentum perpendicular to the beam axis) of the charged lepton has the characteristic Jacobian edge at half the mass of  $W$  boson. In practice, electroweak radiative corrections modify the lepton  $p_T$  spectrum, mainly due to the emission of photons from the decay lepton. If no correction was applied for this radiative process, the  $m_W$  measurement would be biased by  $\approx 200$  MeV [7]. Throughout this paper, we use the convention  $\hbar = c = 1$ .

In the first Run II measurement [7] of  $W$  boson mass, WGRAD [8] and ZGRAD [9] programs were used to calculate the QED radiative correction. WGRAD and ZGRAD are exact next-to-leading order (NLO) electroweak matrix element calculations of the  $q\bar{q} \rightarrow W\gamma \rightarrow l\nu\gamma$  and  $q\bar{q} \rightarrow Z\gamma \rightarrow \bar{l}l\gamma$  processes, respectively. The effect of higher-order radiative corrections has been estimated to be about 10% [7, 10] of  $W$  boson mass shift estimated from these NLO calculations. In order to increase the precision of the QED radiative correction for  $W$  boson mass measurement, higher-order calculations were used, as implemented in HORACE [10–14] and PHOTOS [15, 16] programs. These programs calculate

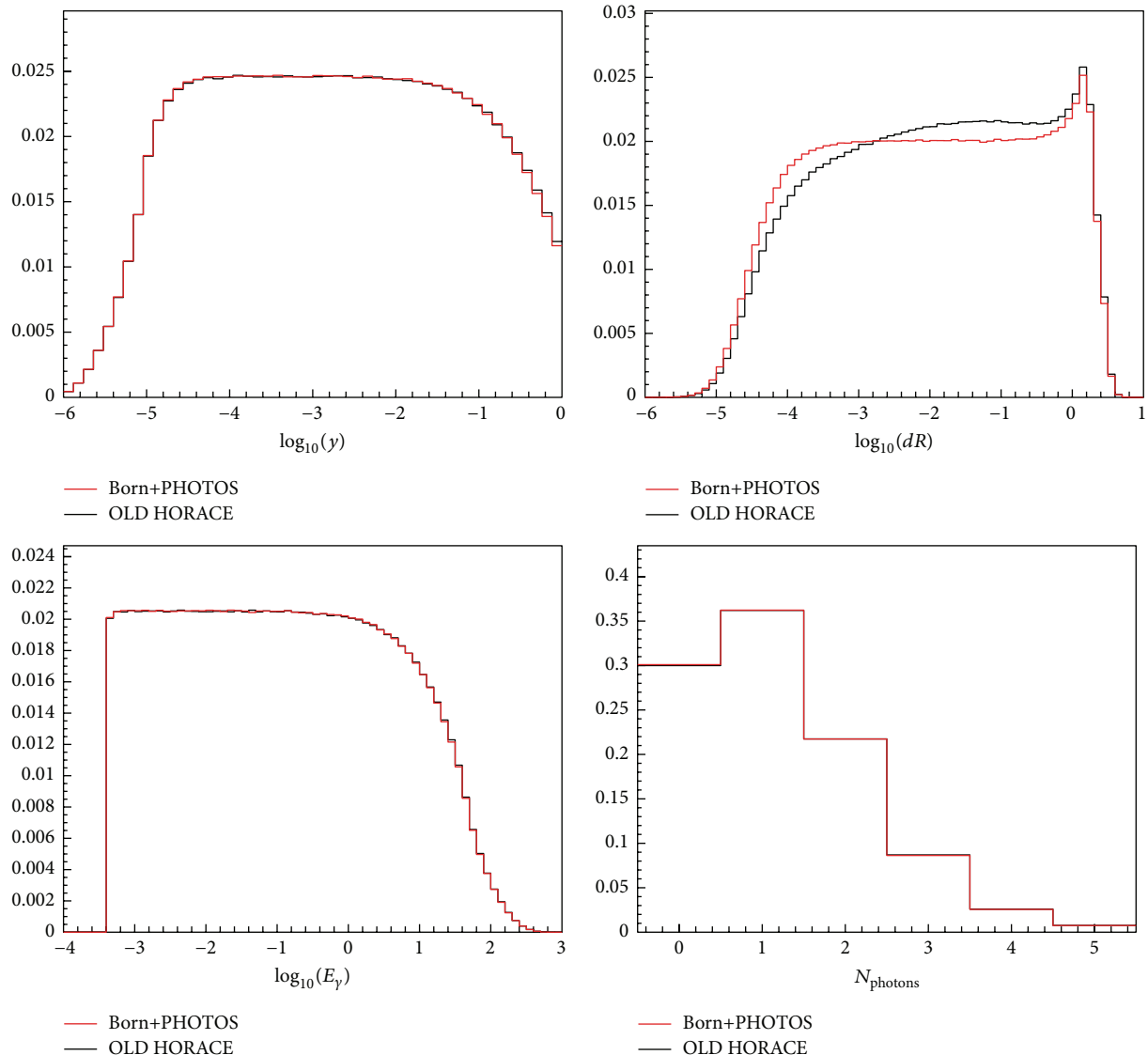


FIGURE 1: Clockwise from top-left: comparisons of the distributions of  $\log_{10}(y_\gamma)$ ,  $\log_{10}(\Delta R(l\gamma))$ ,  $n_\gamma$ , and  $\log_{10}(E_\gamma/\text{GeV})$  for the  $\gamma^*/Z \rightarrow e^+e^- + n\gamma$  process between the “Born” mode of OLD HORACE interfaced with PHOTOS and OLD HORACE in the exponentiation mode. The smaller of the two  $\Delta R$  values with respect to the two electrons is shown.

the emission of multiple photons with the appropriate rates, energy, and angular distributions.

PHOTOS uses the exact first-order matrix element of  $W$  and  $Z$  boson decay for the photon emission kernel. For multiphoton radiation, PHOTOS uses an iterative solution for this kernel, developed on the basis of an exact and complete phase space parametrization. This ensures not only resummation of leading-logarithm contributions of higher orders but also the infrared region of the phase space being accurately simulated [16] (Z. Was, private communication).

HORACE is a parton-level electroweak Monte Carlo generator for precision simulations of charged-current and neutral-current Drell-Yan processes. HORACE uses the full phase space for each radiated photon and there is no ordering of the photons (i.e., in angle or transverse momentum) in multiphoton emission (C. M. Carloni Calame, G. Montagna,

and A. Vicini, private communication). Two versions of the HORACE program are available. The OLD version [10, 11] implements a multiphoton emission QED parton shower algorithm for the simulation of final-state radiation (FSR) in the leading-logarithmic approximation, without initial-state radiation (ISR) and without interference between ISR and FSR. In this sense the OLD HORACE program is similar to the PHOTOS program, which also implements multiphoton FSR. OLD HORACE does not include full one-loop electroweak corrections, but it mimics the real radiation matrix element for the description of the photon radiation in  $W$  and  $Z$  boson decays, in the leading-logarithmic approximation (C. M. Carloni Calame, G. Montagna, and A. Vicini, private communication). There is also a NEW HORACE program [12, 13], which implements multiphoton ISR and FSR with interference and also matches each photon to the exact matrix

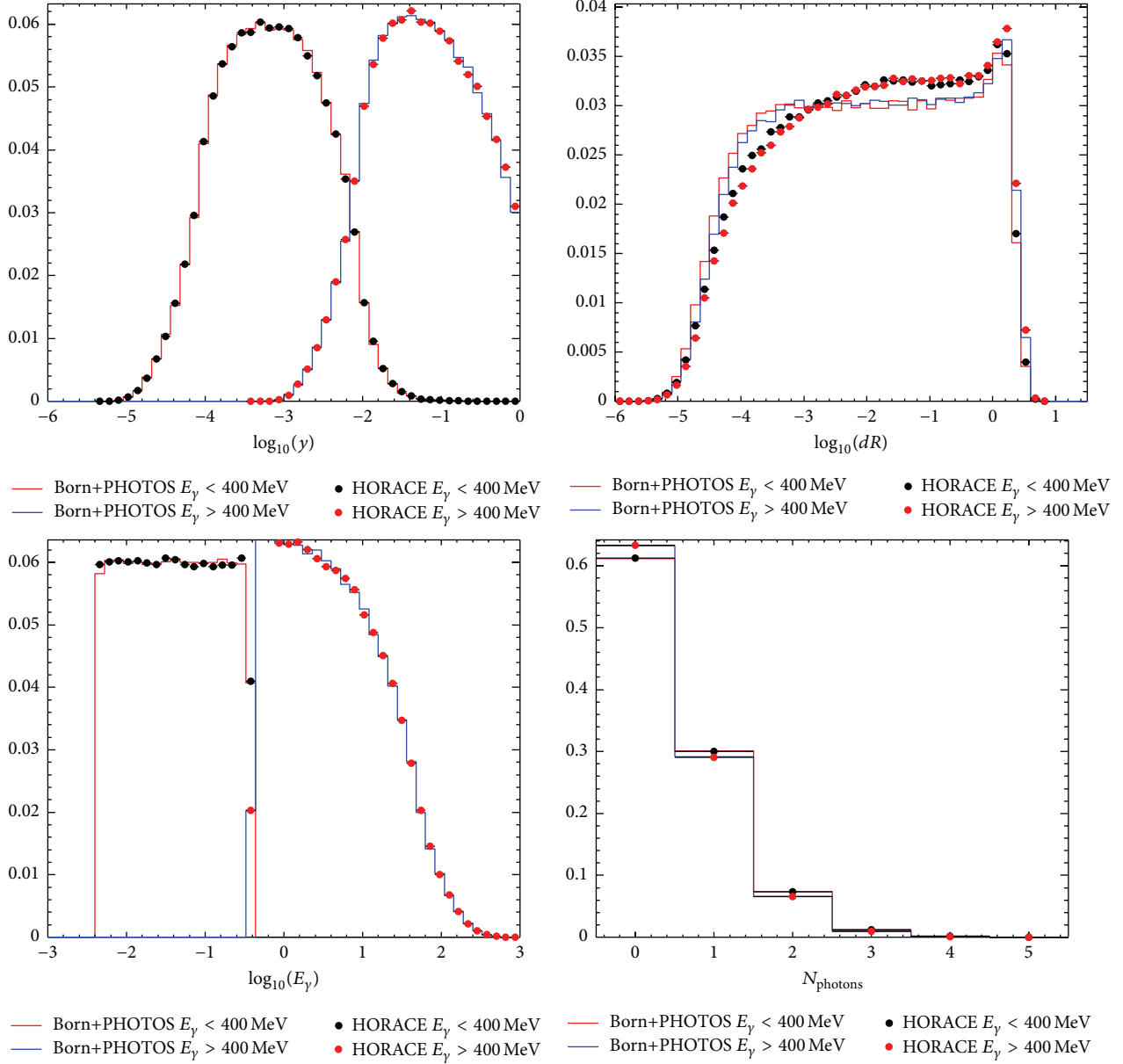


FIGURE 2: Clockwise from top-left: comparisons of the distributions of  $\log_{10}(y)$ ,  $\log_{10}(\Delta R(l\gamma))$ ,  $n_\gamma$ , and  $\log_{10}(E_\gamma/\text{GeV})$  for the  $\gamma^*/Z \rightarrow e^+e^- + n\gamma$  process between the “Born” mode of OLD HORACE interfaced with PHOTOS and OLD HORACE in the exponentiation mode. The comparisons are shown separately for low ( $E_\gamma < 400$  MeV) and high-energy ( $E_\gamma > 400$  MeV) photons. The smaller of the two  $\Delta R$  values with respect to the two electrons is shown.

element calculation of one-loop electroweak corrections and single-photon emission (C. M. Carloni Calame, G. Montagna, and A. Vicini, private communication).

The PHOTOS program provides a generic interface to any other event generator such that all charged leptons produced by the latter can be passed through the PHOTOS FSR algorithm. We use this feature as follows. We generate  $W$  and  $Z$  boson events for Tevatron  $p\bar{p}$  collisions at  $\sqrt{s} = 1.96$  TeV, including higher-order QCD matrix elements and

QCD resummation effects, but without loops or emission of electroweak bosons. We interface these events to PHOTOS such that the events from the chain contain the QED-FSR photons added by PHOTOS. We save photons with  $p_T > 0.4$  MeV and the events are processed with a detector simulation [6, 7] to make the pseudodata and the mass-fitting templates. Lowering the photon  $p_T$  threshold further has negligible effect on the results presented here, within the uncertainties quoted.

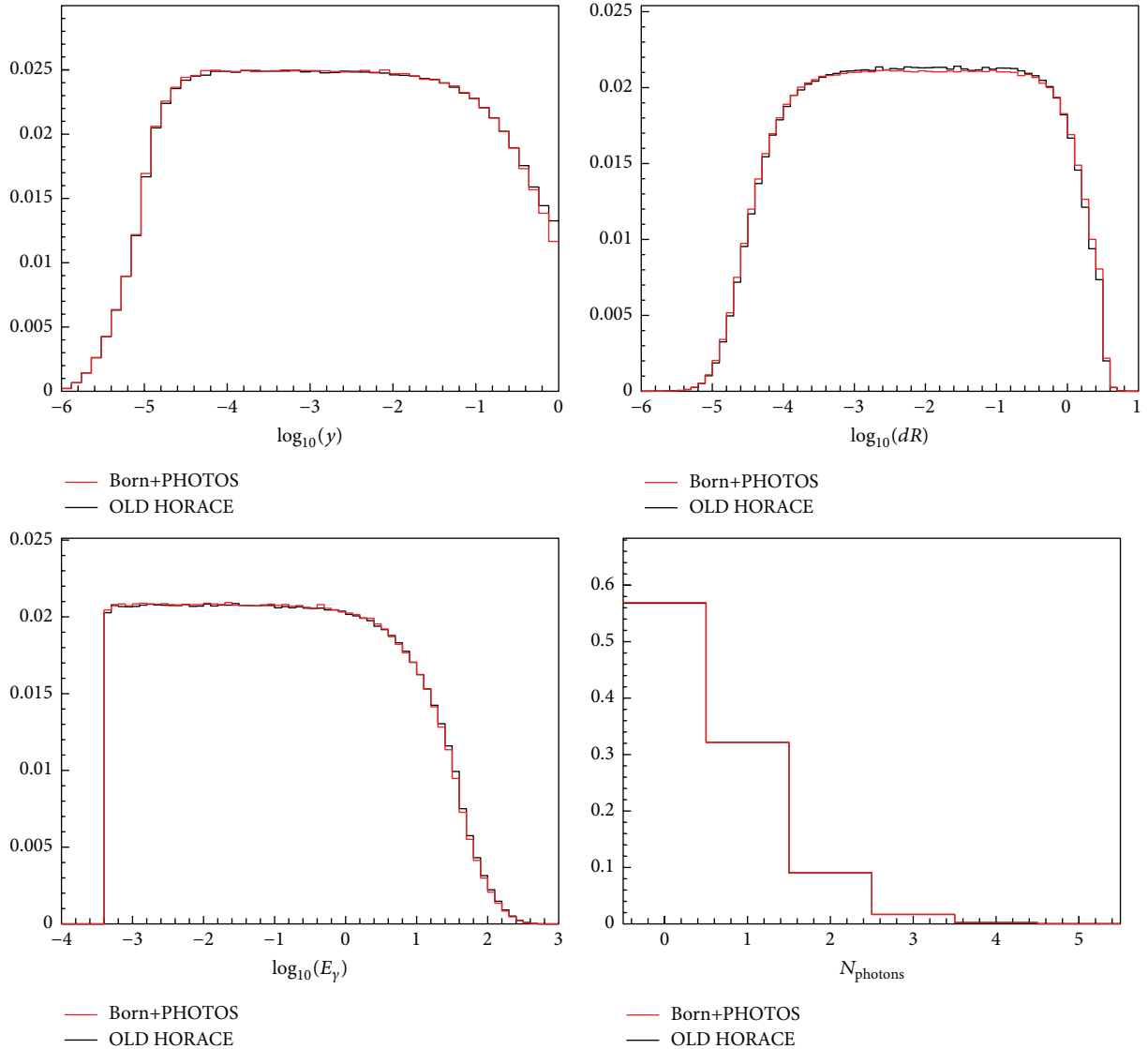


FIGURE 3: Clockwise from top-left: comparisons of the distributions of  $\log_{10}(y_\gamma)$ ,  $\log_{10}(\Delta R(l\gamma))$ ,  $n_\gamma$ , and  $\log_{10}(E_\gamma/\text{GeV})$  for the  $W^+ \rightarrow e^+ \nu + n\gamma$  process between the “Born” mode of OLD HORACE interfaced with PHOTOS and OLD HORACE in the exponentiation mode. The  $\Delta R$  is computed with respect to the positron.

In this paper we present comparisons between the distributions and the mass-fitting results obtained from the OLD HORACE and PHOTOS programs.

## 2. Electron Channel Comparisons

To make direct comparisons between quantities sensitive to QED physics, we need to ensure that the underlying boson and lepton distributions are identical between OLD HORACE and PHOTOS. For this purpose we use the “Born” mode of OLD HORACE to generate Born-level  $q\bar{q} \rightarrow W \rightarrow l\nu$  and  $q\bar{q} \rightarrow \gamma^*/Z \rightarrow \bar{l}l$  events, which are then processed through PHOTOS. The Born mode generates these purely  $2 \rightarrow 1 \rightarrow 2$  parton processes with no radiative photons. These events are compared with events from OLD HORACE run in

the QED multiphoton emission FSR mode. Both OLD HORACE and PHOTOS are run in the “exponentiation” mode, which exercises their full physics content. All of the events used in these comparisons have unit weights. For all generated events we make a generator-level cut on the partonic center-of-mass energy  $\sqrt{s} > 40 \text{ GeV}$  to remove the contribution of the photon pole for neutral-current events. For consistency, we also apply this cut on the charged-current events.

In Figure 1 we compare the distributions for photon emission rates as well as the energy and angular distributions for the  $\gamma^*/Z \rightarrow e^+e^- + n\gamma$  process. For these comparisons we consider photons with energy  $E_\gamma > 0.4 \text{ MeV}$ ; photons with lower energy than this threshold are not counted and ignored in the distributions. In addition to the number  $n_\gamma$  of photons emitted, we find that the distributions of the

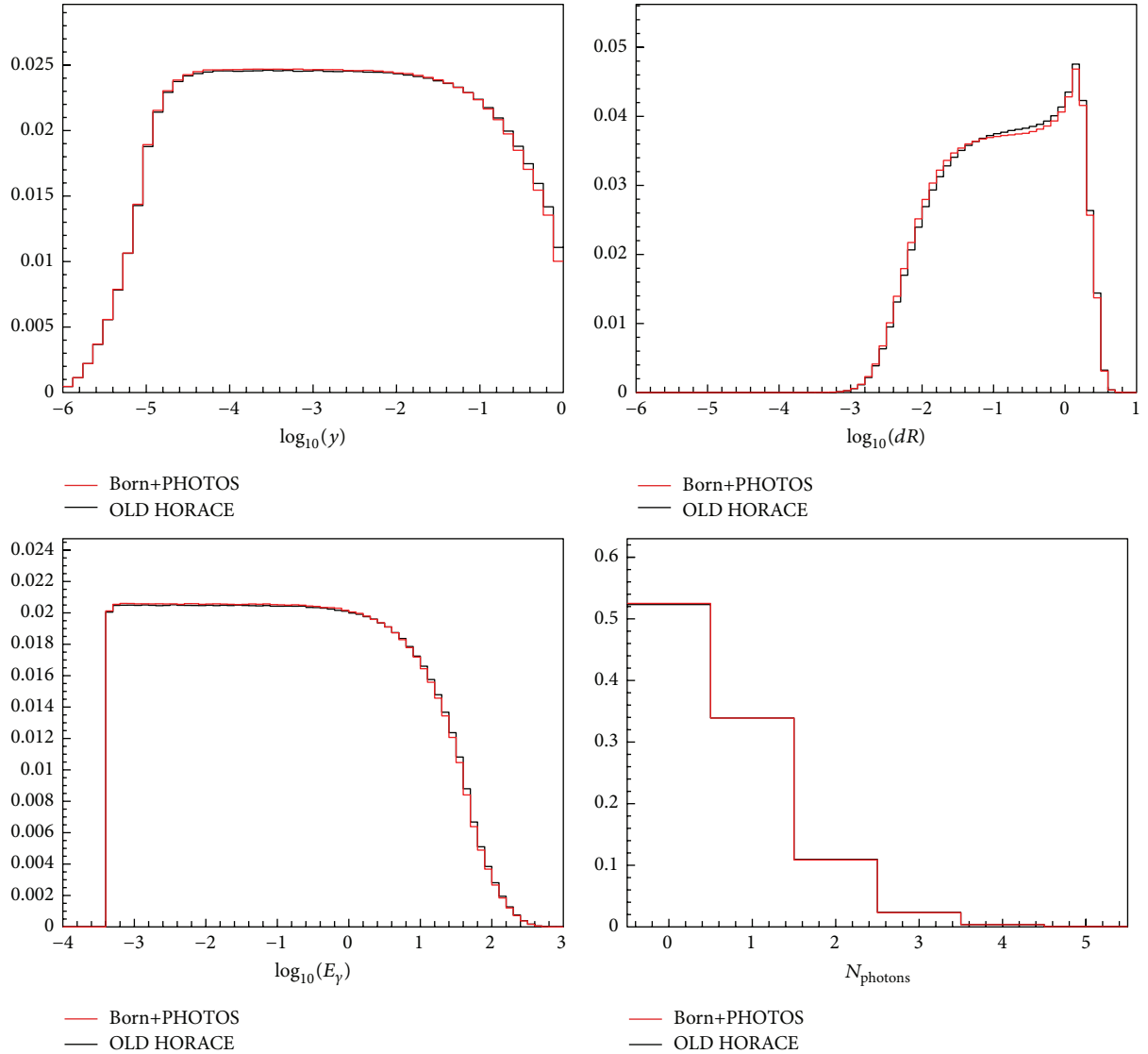


FIGURE 4: Clockwise from top-left: comparisons of the distributions of  $\log_{10}(y)$ ,  $\log_{10}(\Delta R(l\gamma))$ ,  $n_\gamma$ , and  $\log_{10}(E_\gamma/\text{GeV})$  for the  $\gamma^*/Z \rightarrow \mu^+\mu^- + n\gamma$  process between the “Born” mode of OLD HORACE interfaced with PHOTOS and OLD HORACE in the exponentiation mode. The smaller of the two  $\Delta R$  values with respect to the two muons is shown.

following quantities are useful to compare:  $\log_{10}(E_\gamma/\text{GeV})$ , the fractional photon energy  $y_\gamma \equiv E_\gamma/(E_\gamma + E_l)$  (where  $E_l$  is the energy of the final-state lepton), and  $\Delta R(l\gamma) \equiv \sqrt{(\Delta\eta_{l\gamma})^2 + (\Delta\phi_{l\gamma})^2}$  (the  $\eta - \phi$  angular separation between a photon and the final-state lepton, where the pseudorapidity  $\eta = -\log[\tan(\theta/2)]$ ,  $\theta$  being the polar angle with respect to the beam axis, and  $\phi$  is the azimuthal angle about the beam axis).

Figure 2 shows the photon distributions separately for low-energy and high-energy photons. The photon energy cut value of 400 MeV is chosen because roughly half of the photons are above and below this cut. These distributions show that the angular distribution is almost independent of

the photon energy, allowing us to draw conclusions from the inclusive photon distributions.

In Figure 3 we compare the photon distributions for the  $W^+ \rightarrow e^+\nu + n\gamma$  process. These distributions are identical for the charge conjugate processes due to the  $p\bar{p}$  collisions at the Tevatron. The comparisons between OLD HORACE and PHOTOS show good agreement in the photon emission rates and the photon energy distributions. For the  $\gamma^*/Z \rightarrow e^+e^- + n\gamma$  process, the photon angular distribution shows about 10% difference at small angles, a difference that is not correlated with photon energy. As we show in Section 4, this difference does not cause a relative shift in the fitted  $Z \rightarrow ee$  mass between the two algorithms.

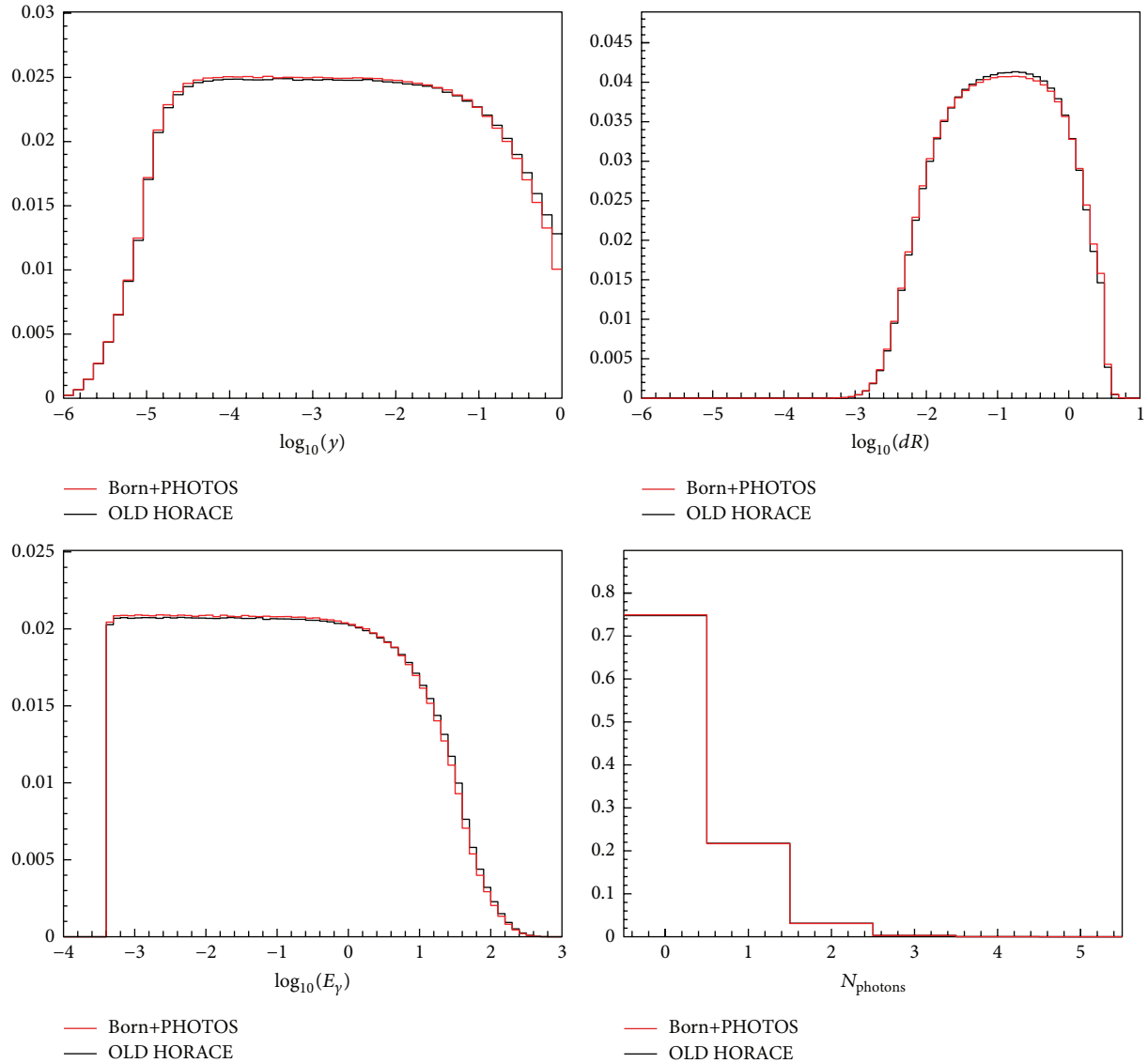


FIGURE 5: Clockwise from top-left: comparisons of the distributions of  $\log_{10}(\gamma)$ ,  $\log_{10}(\Delta R(l\gamma))$ ,  $n_\gamma$ , and  $\log_{10}(E_\gamma/\text{GeV})$  for the  $W^+ \rightarrow \mu^+ \nu + n\gamma$  process between the “Born” mode of OLD HORACE interfaced with PHOTOS and OLD HORACE in the exponentiation mode. The  $\Delta R$  is computed with respect to the muon.

### 3. Muon Channel Comparisons

We repeat the above comparisons for the muon channel. In Figures 4 and 5 we compare the distributions for photon emission rates as well as the energy and angular distributions for the  $\gamma^*/Z \rightarrow \mu^+ \mu^- + n\gamma$  and  $W^+ \rightarrow \mu^+ \nu + n\gamma$  processes, respectively. Figure 6 shows the photon distributions separately for low-energy and high-energy photons. The rates and distributions are in good agreement between OLD HORACE and PHOTOS for the muon channel.

The photon emission at wide angle to the lepton is similar between the muon and electron channels, for both the energy and angular distributions. In the collinear region the photon emission off muons is highly suppressed due to the larger muon mass. This also reduces the number of photons emitted

per event for the muon channel, relative to the electron channel.

### 4. Mass Fits

We quantify the impact of the small differences in photon rates and distributions between OLD HORACE and PHOTOS in terms of shifts in the fitted  $W$  boson masses. For this purpose, we propagate high-statistics OLD HORACE and PHOTOS samples through the parameterized CDF detector simulation used in  $W$  boson mass measurement [6]. We generate templates and pseudodata from both samples and perform the mass fits to these pseudodata using these templates, in the same manner that templates are used to fit the collider data [3–6].

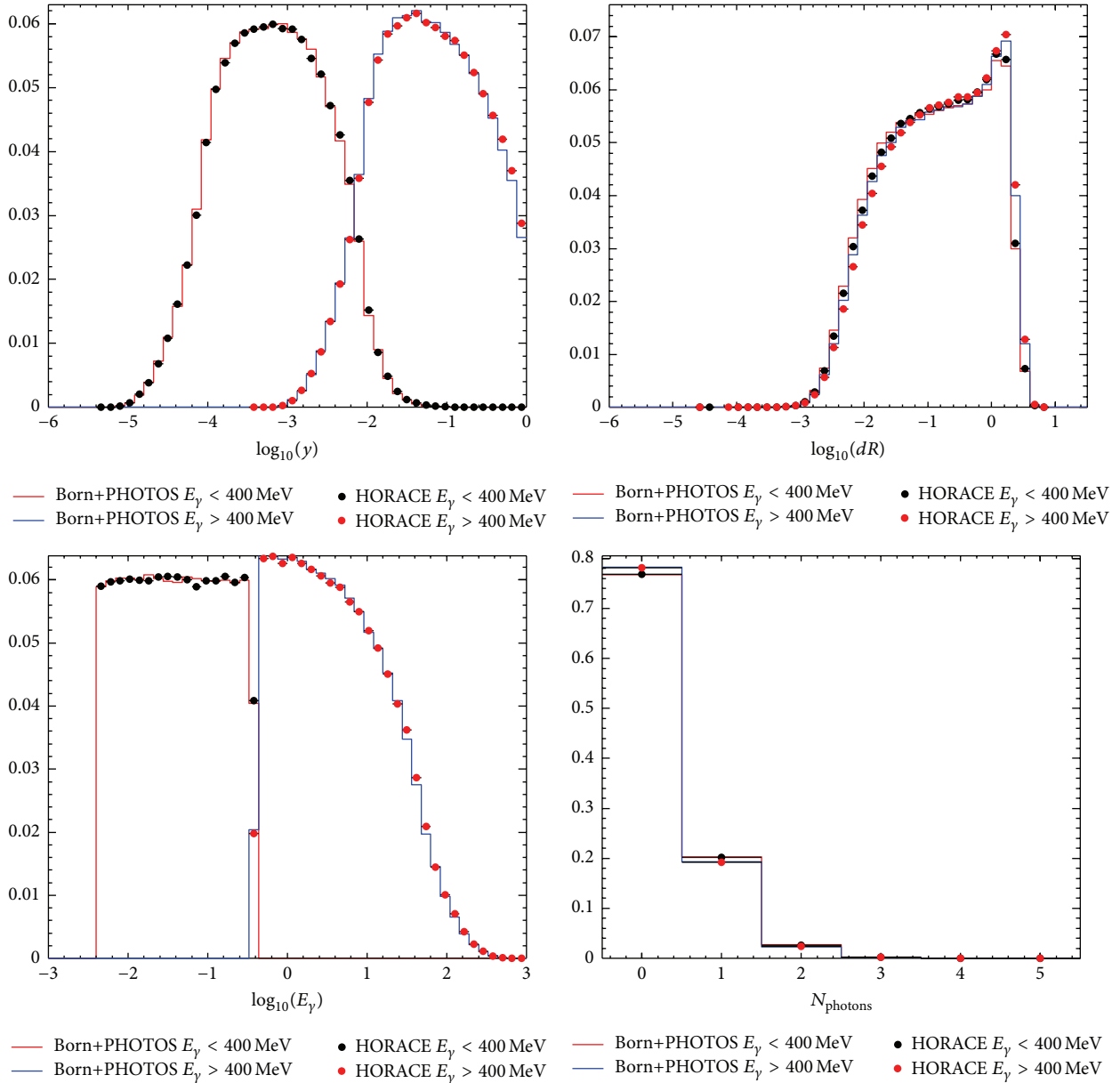


FIGURE 6: Clockwise from top-left: comparisons of the distributions of  $\log_{10}(y)$ ,  $\log_{10}(\Delta R(l\gamma))$ ,  $n_\gamma$ , and  $\log_{10}(E_\gamma/\text{GeV})$  for the  $\gamma^*/Z \rightarrow \mu^+\mu^- + n\gamma$  process, separated into low ( $E_\gamma < 400$  MeV) and high-energy ( $E_\gamma > 400$  MeV) photons. The smaller of the two  $\Delta R$  values with respect to the two muons is shown.

We perform fits to the distributions of transverse quantities in  $W$  boson events: the charged lepton  $p_T$ , neutrino  $p_T$ , and transverse mass  $m_T$ . The transverse mass is defined as  $m_T = \sqrt{2p_T^\ell p_T^\nu (1 - \cos \Delta\phi)}$ , where  $\Delta\phi$  is the azimuthal angle between the charged lepton and neutrino momenta in the transverse plane. In the electron channel, we also perform a fit to the ratio of electron calorimeter energy to track momentum ( $E/p$ ), which is used by the CDF experiment to obtain the calorimeter calibration using the electron track. In  $Z$  boson events, we fit the distributions of  $Z$  boson invariant-mass obtained from electron calorimeter deposition measurements (cluster mass) and from track

momentum measurements of electrons and muons (track mass).

We obtain the difference between the mass fits to the HORACE pseudodata and the PHOTOS pseudodata which quantifies the relevant differences between the two QED codes. Tables 1 and 2 show the differences along with their statistical uncertainties. Table 1 uses PHOTOS templates and is essentially identical to Table 2 which uses HORACE templates. The two tables provide validation that the comparison of the two pseudodata samples does not depend on the template choice, as long as the same templates are used for the fits being compared.



TABLE 1: Difference between HORACE and PHOTOS pseudodata in fitted masses. The shift in the dimensionless  $E/p$  value has been multiplied by 80 GeV to convert to the equivalent shift in the fitted  $W$  boson mass. Templates were made using PHOTOS. The statistical errors are shown. The templates and pseudodata use 10 billion events at the generator level as the input to the detector simulation.

Fit type	$m_{\text{horace}} - m_{\text{photos}}$ (MeV)	
	Electron	Muon
$W$ transverse mass	$0.0 \pm 0.6$	$0.0 \pm 0.4$
$W$ lepton $p_T$	$-0.4 \pm 0.4$	$0.0 \pm 0.4$
$W$ neutrino $p_T$	$0.6 \pm 0.8$	$1.4 \pm 0.6$
$W$ $E/p$	$0.4 \pm 0.1$	—
$Z$ cluster mass	$0.2 \pm 0.4$	—
$Z$ track mass	$-1.0 \pm 0.6$	$-0.8 \pm 0.3$

TABLE 2: Difference between HORACE and PHOTOS pseudodata in fitted masses. Templates were made using HORACE. The shift in the dimensionless  $E/p$  value has been multiplied by 80 GeV to convert to the equivalent shift in the fitted  $W$  boson mass. The statistical errors are shown. The templates and pseudodata use 10 billion events at the generator level as the input to the detector simulation.

Fit type	$m_{\text{horace}} - m_{\text{photos}}$ (MeV)	
	Electron	Muon
$W$ transverse mass	$0.0 \pm 0.6$	$0.2 \pm 0.4$
$W$ lepton $p_T$	$-0.6 \pm 0.4$	$0.0 \pm 0.4$
$W$ neutrino $p_T$	$0.6 \pm 0.8$	$1.6 \pm 0.6$
$W$ $E/p$	$0.4 \pm 0.1$	—
$Z$ cluster mass	$0.0 \pm 0.4$	—
$Z$ track mass	$-1.2 \pm 0.7$	$-0.8 \pm 0.3$

The lepton track momentum is more sensitive to photon emission as compared to the calorimeter cluster energy. Radiated FSR photons directly subtract from the track momentum. The electron calorimeter cluster absorbs most of the photon radiation and is therefore less sensitive to the emission pattern. The comparison of the  $Z \rightarrow ee$  mass shift obtained from the calorimeter cluster and the track measurements provides an additional, sensitive test of the two programs.

## 5. Conclusions

We find that the QED generators OLD HORACE and PHOTOS agree with each other in the photon rates and distributions. The only noticeable difference is in the photon angular distribution for the  $\gamma^*/Z \rightarrow e^+e^- + n\gamma$  process, at small angular separation from the nearest lepton. We quantify the comparison by computing relative  $W$  and  $Z$  boson mass shifts and find them to be consistent with  $\approx 0.7$  MeV within statistical uncertainties. We conclude that a systematic uncertainty of 0.7 MeV would account for any differences in the FSR multiphoton emission between the HORACE and PHOTOS algorithms.

## Competing Interests

The authors declare that they have no competing interests.


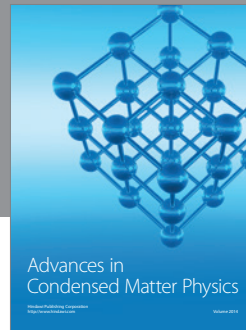
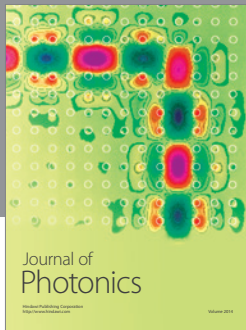
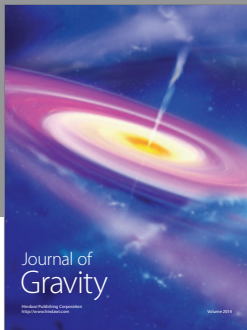
## Acknowledgments

The authors wish to thank Ilija Bizjak for his assistance with the HORACE program and Zbigniew Was for providing the interface to the PHOTOS program. The authors wish to thank William Ashmanskas, Franco Bedeschi, Daniel Beecher, Ilija Bizjak, Kenichi Hatakeyama, Christopher Hays, Mark Lancaster, Sarah Malik, Larry Nodulman, Peter Renton, Tom Riddick, Ravi Shekhar, Melvyn Shochet, Oliver Stelzer-Chilton, Siyuan Sun, David Waters, Yu Zeng, and other colleagues in the CDF Collaboration for helpful discussions. They also thank Carlo Carloni Calame, Guido Montagna, Alessandro Vicini, Doreen Wackerroth, and Zbigniew Was for discussions regarding electroweak radiative corrections. They acknowledge the support of the U.S. Department of Energy, Office of High Energy Physics, and the Fermi National Accelerator Laboratory (Fermilab). The computational resources used in this study were provided by Fermilab. Fermilab is operated by Fermi Research Alliance, LLC, under Contract no. DE-AC02-07CH11359 with the United States Department of Energy.

## References

- [1] M. Baak, J. Cúth, J. Haller et al., “The global electroweak fit at NNLO and prospects for the LHC and ILC,” *The European Physical Journal C*, vol. 74, article 3046, 2014.
- [2] T. Aaltonen, V. M. Abazov, B. Abbott et al., “Combination of CDF and D0  $W$ -Boson mass measurements,” *Physical Review D*, vol. 88, no. 5, Article ID 052018, 11 pages, 2013.
- [3] T. Aaltonen, B. A. González, S. Amerio et al., “Precise measurement of the  $W$ -boson mass with the CDF II detector,” *Physical Review Letters*, vol. 108, no. 15, Article ID 151803, 2012.
- [4] V. M. Abazov, B. Abbott, B. S. Acharya et al., “Measurement of the  $W$  Boson Mass with the D0 Detector,” *Physical Review Letters*, vol. 108, Article ID 151804, 2012.
- [5] V. M. Abazov, B. Abbott, B. S. Acharya et al., “Measurement of the  $W$  boson mass with the D0 detector,” *Physical Review D*, vol. 89, no. 1, Article ID 012005, 2014.
- [6] T. Aaltonen, S. Amerio, D. Amidei et al., “Precise measurement of the  $W$ -boson mass with the collider detector at Fermilab,” *Physical Review D*, vol. 89, no. 7, Article ID 072003, 2014.
- [7] T. Aaltonen, A. Abulencia, J. Adelman et al., “First run II measurement of the  $W$  boson mass at the Fermilab Tevatron,” *Physical Review D*, vol. 77, Article ID 112001, 2008.
- [8] U. Baur, S. Keller, and D. Wackerroth, “Electroweak radiative corrections to  $W$  boson production in hadronic collisions,” *Physical Review D*, vol. 59, no. 1, Article ID 013002, 18 pages, 1999.
- [9] U. Baur, O. Brein, W. Hollik, C. Schappacher, and D. Wackerroth, “Electroweak radiative corrections to neutral-current Drell-Yan processes at hadron colliders,” *Physical Review D*, vol. 65, no. 3, Article ID 033007, 2002.
- [10] C. M. Carloni Calame, G. Montagna, O. Nicrosini, and M. Treccani, “Higher-order QED corrections to  $W$ -boson mass

- determination at hadron colliders,” *Physical Review D*, vol. 69, no. 3, Article ID 037301, 2004.
- [11] C. M. Carloni Calame, G. Montagna, O. Nicrosini, and M. Treccani, “Multiple photon corrections to the neutral-current Drell-Yan process,” *Journal of High Energy Physics*, vol. 2005, article 019, 2005.
- [12] C. M. Carloni Calame, G. Montagna, O. Nicrosini, and A. Vicini, “Precision electroweak calculation of the charged current Drell-Yan process,” *Journal of High Energy Physics*, vol. 2006, no. 12, article 16, 2006.
- [13] C. M. Carloni Calame, G. Montagna, O. Nicrosini, and A. Vicini, “Precision electroweak calculation of the production of a high transverse-momentum lepton pair at hadron colliders,” *Journal of High Energy Physics*, vol. 2007, no. 10, article 109, 2007.
- [14] HORACE version 3.1, <http://www2.pv.infn.it/~hepcomplex/horace.html>.
- [15] E. Barberio and Z. Wař, “PHOTOS—a universal Monte Carlo for QED radiative corrections: version 2.0,” *Computer Physics Communications*, vol. 79, no. 2, pp. 291–308, 1994.
- [16] A. B. Arbuzov, R. R. Sadykov, and Z. Was, “QED bremsstrahlung in decays of electroweak bosons,” *The European Physical Journal C*, vol. 73, no. 11, article 2625, 18 pages, 2013.



**Hindawi**

Submit your manuscripts at  
<http://www.hindawi.com>

